Continuous crossover from the dilute to semidilute concentration regime in spherically confined polymers

*Peter Cifra and Tomáš Bleha**

Polymer Institute, Slovak Academy of Sciences, 84541 Bratislava, Slovakia

ToC

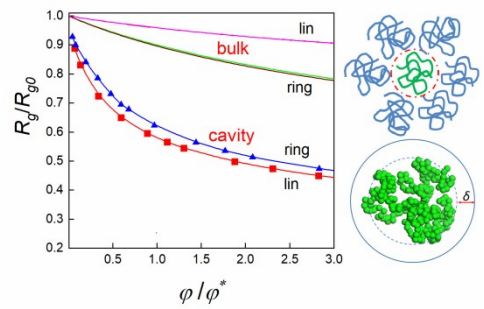

ABSTRACT: We present results of simulations of flexible polymers in a sphere that show a steady reduction of the chain dimension with concentration. The 3D confinement leads to a 40 % shrinking of the chain size at the overlap concentration φ^*. The chain squeezing is intensified by the polymer depletion inside a sphere evaluated by a novel formula. The depletion induces the accumulation of polymers in the cavity center. Because this effect is ignored in the scaling theory, its predictions are not fully consistent with the simulation results. We provide the validation arguments that the shrinking of coils packed at the threshold φ^* in bulk solution is comparable to the squeezing of polymers in a cavity. The size contraction by about 10 % at φ^* in ring polymers in bulk lies midway between those for the linear polymers in bulk and confined polymers, in harmony with the free-energy penalty for penetration of surrounding restraints.

INTRODUCTION

Polymers are often found in spaces much smaller than their natural size. An entrapment of polymers inside closed cavities of the spherical or comparable native shapes gives rise to quite strong confinement effects. The polymers in nano/microscale compartments are widely encountered in the biological milieu, for example, in sub-cellular structures or protein capsids. The confinement effects are common in biomimetic cavities produced by encapsulation of polymers such as enzymes, or polymer-drug conjugates into a shell.[1] Soft artificial vesicles mimicking cell membranes, on the base of lipids (liposomes) or block copolymers, represent alternative variants of polymer nanoparticles for transport and targeted drug delivery.[2-3] A droplet of polymer solution is an elementary realization of a cavity entrapment. Such droplets in aerosols are used in mass spectroscopy to analyze complex macromolecules.[4] In reverse micelles, the nanoscopic droplets of water solution of polymers can be uniformly distributed within a nonpolar solvent.[5] The polymers in biological or biomimetic systems are often grown in cavities.[6] Hence, apart from polymers and solvents, the cavities may contain monomers and other small crowding molecules.[7]

Since the conformational space available to polymers is severely restricted on confinement, their structure, and properties in cavities may differ from those in bulk. The understanding of chain organization in the cavity interior underlies a proper design of artificial polymer cavity structures. In this respect, the influence of concentration on the behavior of polymers inside a cavity is of primary interest. In bulk solution, this influence is described by the scaling theory that presumes for flexible polymers three concentration regimes: dilute, semidilute, and concentrated.[8-9] The first two regimes are divided by the critical overlap volume fraction of

polymer φ^*, a key quantity in the theory of polymer solutions. In the dilute regime, the polymer coils are separated from each other, whereas they overlap and interpenetrate in the semidilute regime.

The scaling theory of linear flexible polymers assumes that in the dilute regime, the radius of gyration R_g is independent of concentration and is given by its value at infinite dilution R_{g0} until the overlap concentration is reached. The size of a swollen coil in semidilute solution is characterized by a correlation length ξ rather than by R_g. The length scale ξ represents the average distance between two entanglement points. Alternatively, in the blob theory[8-9], ξ gives the mean size of a blob within which the polymer behaves as an independent coil. In the semidilute regime, the theory predicts the dependence $\xi \sim \varphi^{-3/4}$ for the correlation length, from which the decrease of polymer dimensions with increasing concentration $R_g \sim \varphi^{-1/8}$ ensues.[8-9]

The confined polymer solutions have been modeled using both theory and simulation.[8-15] In slit and channel geometries, the chain conformations and the concentration regimes are mainly affected by the anisotropy of the confining surface. For example, the regimes of pancake-like or cigar-like conformations of pronounced longitudinal dimensions were predicted to emerge at strong confinement in the slit and channel geometries, respectively.[8-13] However, the scaling description of a polymer inside an isotropic spherical cavity[11, 16-20] differs from that for slits and channels as the polymer concentration in a closed cavity increases with the cavity compression.

Besides, the presence of the repulsive confining surface gives rise to an inhomogeneous distribution of polymer segments in solutions. Since polymers have less conformational entropy close to the surface, a layer of polymer depletion (negative adsorption) of the thickness δ arises near a surface.[21] The non-uniform polymer distribution is mostly neglected in the current theories of confined polymer solutions. Nonetheless, the scaling expressions for the free energy due to the surface depletion of a linear chain confined inside a sphere have been presented.[22]

To shed light on the conformation of polymers and their distribution in solution in the interior of artificial and biological cavities, vesicles, and droplets, we simulated in the present paper the linear and ring flexible polymers entrapped in good solvent in a sphere. We focus on exploring how the radius of gyration R_g and the monomer distribution profile $\rho(r)$ change with polymer concentration in the vicinity of the overlap concentration φ^*. A considerable reduction of the chain dimensions with concentration observed even below the threshold φ^* is associated with a wide depletion layer arising near the cavity surface. We demonstrate that shrinking of the close-packed coils at the overlap threshold φ^* in bulk solution is qualitatively like chain squeezing in a cavity.

SIMULATION MODEL

The Monte Carlo (MC) simulation method used in earlier reports[15, 20, 23-24] is employed to compute the properties of single flexible polymers in a good solvent entrapped in an impenetrable spherical cavity of the effective radius R. The polymer is modeled by the bead-spring model of partially fused spherical beads of $N = 300$ and the radius σ connected by bonds of the effective mean length l (Figure 1). The potential energy U of the system is given by contributions from the bond deformation U_{FENE}, nonbonded interactions between beads U_{nb}, and the bead-cavity wall interaction U_w. Only steric repulsion is accounted for in the two latter potentials. The potential U_w operates between chain segments and the wall in a sphere of radius R^*. Due to a hard wall potential used in simulation, the wall-bead excluded volume interactions diminish the volume of the cavity accessible to a polymer. Following the approach used for a channel[25], we use the bead radius, equivalent to the half-width of the polymer backbone, to define the effective cavity radius $R = R^* - \sigma$.

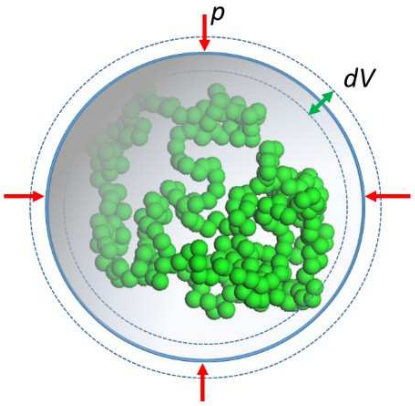

Figure 1. Scheme of the simulation system. The sphere is compressed by the fixed applied pressure p and its volume fluctuates by a small random change dV.

The simulation was performed by the MC protocol employed earlier[20] to evaluate the pressure of polymers inside a sphere. The protocol[20] was designed in analogy with the piston technique for a tube channel.[23,24] In the constant pressure ensemble (NpT) employed, the applied pressure p is fixed in the simulation, and the average value of the radius R is computed. The choice of an NpT ensemble differentiates our approach from the previous simulation studies of polymers inside a sphere based on the NVT ensemble.[16-17, 26] The applied pressure expressed in the dimensionless form pl^3/kT determines the pressure of the polymer exerted on the inner surface of the cavity. The equilibrium conformations of a confined polymer are sampled by using the Metropolis algorithm at constant temperature $kT/\varepsilon = 1$, where ε is the interaction energy parameter in the nonbonded potential U_{nb}.[20, 27] The Boltzmann factor in the Metropolis scheme includes an extra volume fluctuation term $-pdV/kT = \left(\frac{pl^3}{kT}\right) dV/l^3$, where $dV = 4\pi R^2 dR$ represents a small random change in the spherical volume (Figure 1). The chain moves in ring polymers include the small random displacement of beads and consequential evaluation of

change in interactions with all beads and walls. In linear chains, also the reptation was applied, as a more effective conformation change attempt.

The effect of concentration on the behavior of a polymer of the constant chain length N is realized in simulation by a weak compression of the cavity radius R. The resulting volume fraction $\varphi = Nv_1/V$, where v_1 is the volume of a single bead, is controlled by the cavity radius R. Due to bead interpenetration, the mean bond length $l = 0.71$ is slightly shorter than the polymer width $2\sigma = 0.78$. The fusion of beads is also accounted for in the calculation of the reduced volume of a single bead $v_1/l^3 = 0.64$. The identical parameters are used for both linear and ring chain topologies. The size of polymers is monitored by the radius of gyration $R_g = \langle R_g^2 \rangle^{1/2}$. The length quantities are mostly presented in the reduced form, such as R/l.

RESULTS AND DISCUSSION

***$R_g(\varphi)$* in a cavity**. We examine in simulation the dilute regime ($R > R_g$), and the portion of the semidilute regime ($R < R_g$) up to the volume fraction $\varphi \approx 0.10$, for polymers of the constant length N trapped in a sphere. The simulated range involves the critical overlap concentration φ^* at a crossover between the dilute and semidilute regimes. The overlap concentration φ^* is defined as the point where the concentration within a given dilute conformation's pervaded volume is equal to the solution concentration. In bulk solution, the overlap concentration is expressed as the local concentration inside a single coil using the radius of gyration R_{g0} in the dilute solution limit. We use the same approach to estimate the threshold φ^* for the overlap of a polymer with a sphere by the formula $\varphi^* = 3Nv_1/(4\pi R_{g0}^3)$.

The computed reduced radius of gyration R_{g0}/l, 15.38 and 12.32, for the linear and ring chains respectively, confirms that an unconfined ring polymer is more compact than a linear one.[28] From the above formula, the values 0.0124 and 0.0241 follow for the respective overlap concentrations φ^*. The cavity compression results in coil contraction and the decrease of R_g. Simultaneously, the polymer concentration (Figure 2) as well as the intra-sphere pressure increase.

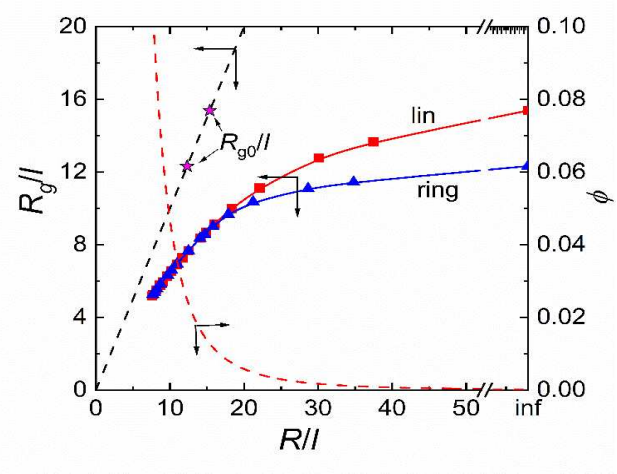

Figure 2. The dependence of the reduced radius of gyration on the reduced radius of a cavity for linear (red squares) and ring (blue triangles) polymers. The respective values R_{g0}/l in the dilute solution limit are indicated by stars. The right ordinate refers to the function $\varphi = 45.86/(R/l)^3$ (dotted line) linking the cavity size and concentration in our model.

In the scaling theory, properties of confined polymers are commonly elucidated by the diagram of regimes showing in the x-y space the regimes of different chain conformations. For a polymer inside a cavity, such a diagram was proposed by using the confinement strength R and chain length N as independent variables.[19] On the other hand, the diagrams of regimes reported for the slit, channel, and box-like confinements[10, 12-13, 29] used the confinement strength R_{g0}/R and

the volume fraction, expressed through the correlation length R_{g0}/ξ as variables. By employing the latter choice, we have constructed the diagram of regimes for a long polymer inside a sphere in a good solvent (Figure 3). Since the variables R_{g0}/R and R_{g0}/ξ in a cavity are not independent, the diagram in Figure 3 involves just lines and the remaining x-y space is irrelevant.

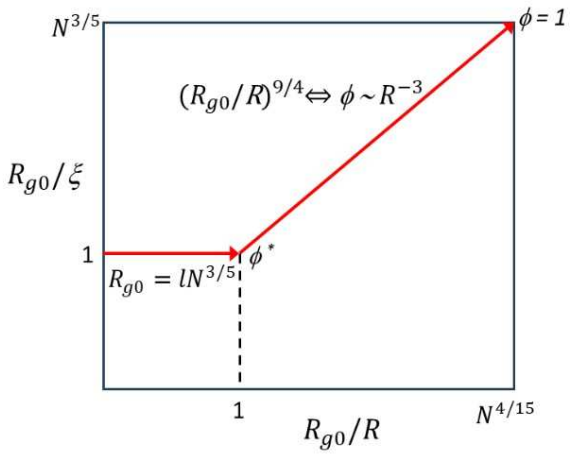

Figure 3. The diagram of regimes for long flexible polymer chains of the constant length N in a sphere where the x-axis expresses the confinement strength, and the y-axis gives a measure of concentration.

The diagram in Figure 3 can be explained by envisioning the blob picture for a chain in a cavity. In the dilute regime, the horizontal line in the diagram corresponds to the constant chain size $R_{g0} \cong lN^{3/5}$ assumed by the theory for a close cavity.[29] In a semidilute solution, the polymer chain consists of independent blobs of diameter ξ filling the cavity. Above φ^*, the compression of chain size R_g in a cavity is controlled by R, hence $R_g \cong R \sim \varphi^{-1/3}$. Considering the decrease of the size of blobs in a good solvent with concentration $\xi \sim \varphi^{-3/4}$, one obtains $R_{g0}/\xi \cong (R_{g0}/R)^{9/4}$ for the line in the semidilute regime. Since $R \cong lN^{1/3}$ applies for the dense globule limit $\varphi = 1$ on the x-axis, the function $R_{g0}/R = N^{4/5}$ is obtained. From the alternative standpoint, the diagram in Figure

3 is equivalent to the simple scaling prediction of the dependence of the correlation length ξ as a function of polymer concentration φ, where $\xi = R_{g0}$ for $R > R_{g0}$, and $\xi \sim \varphi^{-3/4}$ for $R < R_{g0}$.

The simple diagram in Figure 3 quite differs from the complex diagrams of regimes for a polymer confined in a slit or a channel[12-13], mainly because the radius R and the concentration φ in the cavity cannot be changed independently. This distinction is also maintained in the plots of the concentration dependence of the chain size qualitatively sketched for various confinement geometries in Figure S1 in SI. The dependence $R_g(\varphi)$ in a cavity resembles the related function in bulk solution, and both qualitatively differ from the functions in a slit and a channel where the anisotropic conformations prevail at strong confinement. The large difference between the overlap concentrations in solutions in bulk, slit, and channel following the order $\phi_b^* < \phi_{sl}^* < \phi_{ch}^*$ has been explained by the alignment of anisotropic chains.[12] Because of the alignment, the confined polymers in slits and channels feel the presence of other chains at higher concentrations than those in bulk. The anisotropic conformations may also emerge at 3D confinement in chains inside the box-like or ellipsoid cavities[29-30], however, at the isotropic confinement in a sphere, the relation $\phi_{sph}^* \cong \phi_b^*$ should apply.

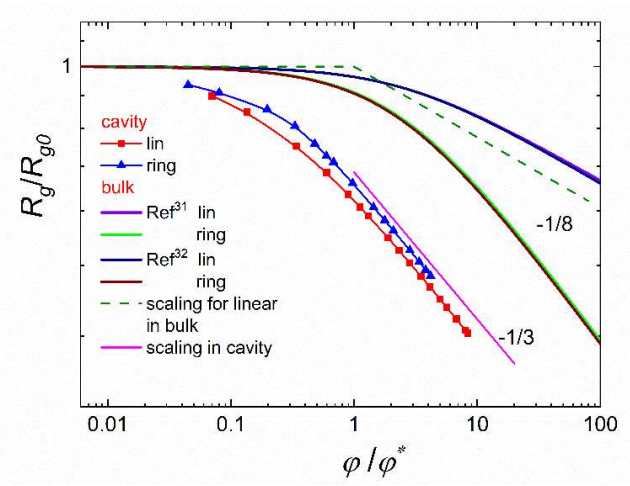

Figure 4. The logarithmic plot of the dependence of the chain size on concentration from simulations of the linear (red squares) and ring (blue triangles) polymers in a cavity plotted using the reduced variables R_g/R_{g0} and φ/φ^*. In addition, the related data from simulations of polymers in bulk solution[31-32] are included (see text and Figure S2). In the scale used, the data of Refs[31-32] for linear and ring polymers, respectively, practically coincide.

Next, the scaling theory depiction of the behavior of polymers near φ^* is compared with the results of the simulation. The change in the polymer dimension with concentration using the reduced variables R_g/R_{g0} and φ/φ^* is shown in Figure S2 and Figure 4 in the linear and logarithmic representations. It is seen that the chain size R_g continuously decreases with concentration even in the large spheres, where $\varphi < \varphi^*$. The polymers in the dilute regime are "aware" of a confining wall, in conflict with the scaling theory assumption of the constant chain size R_{g0} in this regime shown in the diagram in Figure 3. The drop in R_g for a given φ is slightly more marked in Figure 4 in linear chains as compared to rings, apparently because the latter is already more compact in an unconfined state.

Moreover, a smooth transition between dilute and semidilute regimes is observed in simulations in Figure 4 and Figure S2, in opposition to a discontinuous crossover expected on theoretical grounds.[29] The ratio R_g/R_{g0} at the overlap transition amounts to only 0.58 and 0.62 for the linear and ring chains, respectively (Figure 4). Thus, the sphere compression induces a substantial concentration effect, bringing about a 40 % shrinking of chain size near $\varphi/\varphi^* = 1$. The slope about $x = -0.26$ in the semidilute regime in Figure 4 deviates from the exponent $x = -0.33$ considered in the diagram of regimes, presumably because of the emergence of the depletion layer (see below) neglected in the scaling theory. These single-chain results should be relevant to confined polymer solutions, since in the semidilute regime, a long chain in a cavity can be

viewed as a system of multiple shorter chains,[17] as long as the polymer concentration remains unchanged.

Density profiles. We will show that the chain squeezing near $\varphi/\varphi^* = 1$ is amplified by the depletion (negative adsorption) of the polymer segments near an impenetrable surface. To evaluate the depletion effect, we compute the profiles of the number density $\rho = N/V$ inside a sphere. The profiles have been normalized to give the value N by their integration over the whole range of volume of the layers at distance r. The radial density profile $\rho(r)$ in Figure 5 gives the relative segment concentration in individual layers situated at the distance r from the sphere surface for ring polymers at concentrations around the threshold φ^*. The values of the unreduced variable r in profiles in Figure 5 are based on the default bond length $l = 0.71$ used in the simulation. The profiles for a confined linear polymer (Figure S3a) are about equivalent to those for the ring analog in Figure 5.

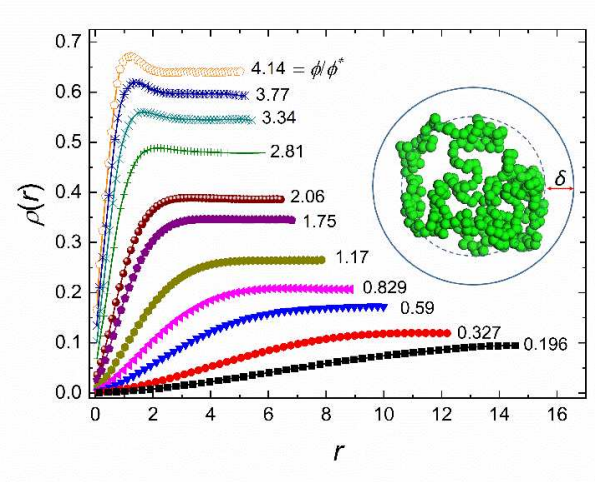

Figure 5. The radial density profiles $\rho(r)$ of a flexible ring polymer in a sphere at the reduced concentrations φ/φ^* given in the legend by taking in simulation $l = 0.71$ for the effective bond length. The snapshot in the inset depicts the chain accumulation due to the depletion effect into the cavity center near $\varphi/\varphi^* = 1$.

Figures 5 and S3a reveal that the sub-surface region, avoided by segments because of the depletion effect, is quite wide. The segments are pushed to the center of a sphere for more available volume and the plateau signaling the uniform filling of segments is formed. In the dilute regime, the constant plateau of the profile $\rho_p(r)$ is restricted to a narrow zone in the cavity center. By increasing concentration, the depletion layer diminishes, and the plateau broadens. These trends in profiles near φ/φ^* in Figures 5 and S3a concur with the single and multiple chain profiles inside a sphere reported for the entire concentration range.[14, 17]

From the profile $\rho(r)$, the thickness of the depletion layer δ may be obtained. Conventionally, the thickness δ is defined through the step profile that would give the same depletion as the continuous profile[21]. This established practice is illustrated in Figure S3b at the estimation of thickness δ in the profile of linear polymer at $\varphi/\varphi^* = 1.29$. The expressions for the calculation of δ are available for the numerous confining geometries of a non-adsorbing polymer such as near a flat wall, in a slit, near a sphere, or between two spheres.[21, 33] In analogy, the depletion thickness δ for a polymer inside a sphere is calculated from the volume V_{ex} excluded by the wall inside a sphere

$$V_{ex} = \frac{4\pi}{3}\left(R^3 - (R-\delta)^3\right) = 4\pi \int_0^R z^2 \left(1 - \frac{\rho(z)}{\rho_p}\right) dz \qquad (1)$$

The profile $\rho(z)$ in the integral is counted from the sphere center, and $z = R - r$. The use of reduced quantities would make eq (1) unwieldy. Therefore, the calculation of V_{ex} by eq (1) is based on profiles from Figure 5 associated with the bond length $l = 0.71$. The number density ρ inside the sphere is normalized in eq (1) by the value of the profile at the plateau ρ_p, instead of the bulk concentration used in common confining geometries.[21] At a closed 3D confinement, the depletion of large spherical shells near the surface ought to increase the segment density in the cavity center.

By conducting the integration in eq (1), the volume V_{ex} excluded by depletion is computed as a function of concentration (Figure 6). The depletion significantly reduces the space accessible to the polymer, whereas the solvent may be distributed in the whole sphere. The effect is pronounced especially in the dilute solution, where the volume V_{ex} of limited accessibility to a polymer amounts to up to two-thirds of the sphere volume. The thickness of the depletion layer δ computed from eq (1) may become up to 30% of the sphere radius (Figure 6, the inset).

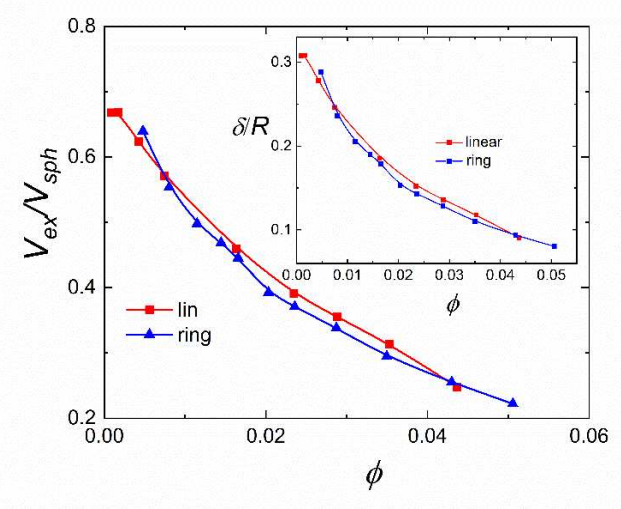

Figure 6. The plot of the reduced accessible volume of a polymer in a cavity as a function of concentration φ. The inset: the analogous function for the relative depletion thickness δ/R.

The dependences of the depletion thickness δ on the sphere radius (Figure S4) or on the concentration (Figure S5) confirm that δ in the cavity is smaller than the size of the unconfined polymer, and the ratio δ/R_{g0} rapidly decreases on sphere compression. Interestingly, in the dilute solution limit, δ/R_{g0} for a linear polymer in a sphere amounts to about 0.75. Hence, the depletion layer under 3D confinement is narrower than in the cases of the less restricting geometries, where $\delta/R_{g0} > 1$ is commonly found.[21, 33]

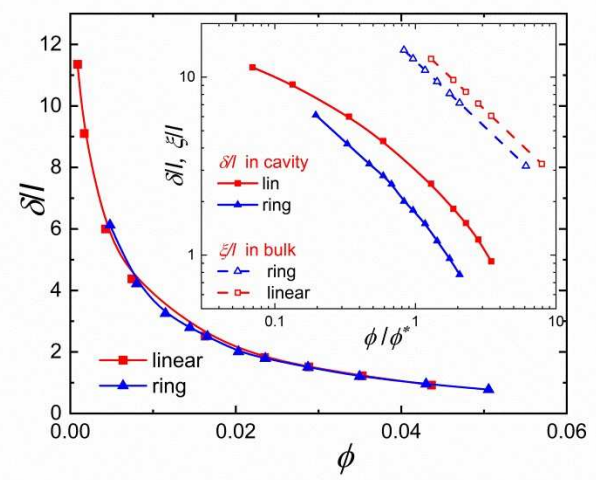

Figure 7. Variation of the reduced depletion thickness δ/l with the concentration φ for flexible linear and ring polymers. The inset: Comparison of the effect of reduced concentration ϕ/ϕ^* on the thickness δ/l in the cavity and the correlation length ξ/l.

Figure 7 shows that the depletion thickness diminishes by increasing concentration even below the threshold φ^*, in an analogous way as observed for the function $R_g(\varphi)$ in Figure 4. According to scaling theory, the depletion thickness δ in the semidilute regime should be equal to the concentration correlation length ξ [8, 33] and follow the power law $\delta \sim \varphi^{-3/4}$. However, the logarithmic plot of the functions $\delta(\varphi)$ for both chain topologies (the inset of Figure 7) suggests steeper slopes, of about -1.1. What is more, the concentration functions $\delta(\varphi)$ in the inset of Figure 7 quite depart from the analogous functions of the correlation length $\xi(\varphi)$. The functions $\xi(\varphi)$ were computed indirectly, using the customary scaling relation of ξ to chain size[9], $\xi = R_{g0}(\varphi/\varphi^*)^{-3/4}$. The observed inconsistency in the concentration dependences of the correlation length and the depletion thickness may cast doubt on the validity of the assumption of $\delta = \xi$ in semidilute solutions under 3D confinement. On the other hand, some arbitrariness in the definition of thickness δ, when the function $\delta(r)$ is replaced by a single value of δ as shown in Figure S3b, may contribute to the disparity encountered in Figure 7.

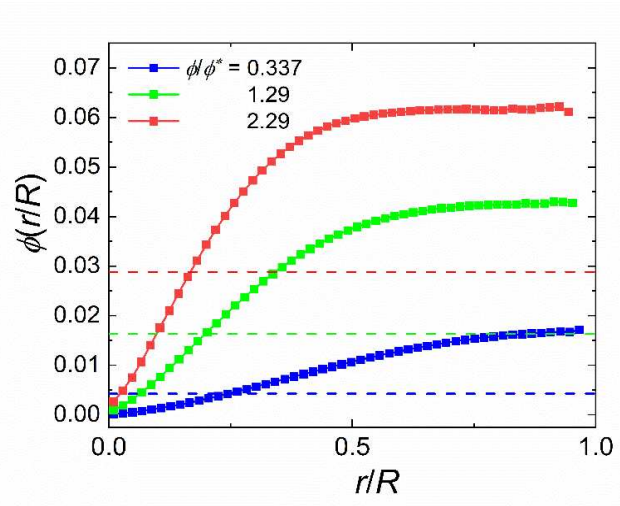

Figure 8. The comparison of the local concentration profiles $\varphi(r)$ (symbols) and the average concentration φ (dotted horizontal lines) for a flexible linear polymer in a sphere at three reduced concentrations φ/φ^*.

A usual disregard of the inhomogeneous spatial distribution of polymer segments inside a cavity in the scaling theory may give rise to some inconsistencies between the theory and simulation. Our results in Figure 8 illustrate the massive discrepancy existing between the average polymer concentration considered in the theory and the actual local concentration in a sphere. A relative increase of the local plateau concentration over the average ones (Figure S6) is particularly conspicuous (about four-fold) in the dilute solution. The plateau and average concentrations for a given N converge at increased concentrations by narrowing the depletion layer. Possibly, the effective segment density in the cavity sub-volume that is primarily filled by a polymer (at $r > \delta$ in Figure S3b) may serve as an alternative concentration descriptor in repulsive cavities.

The simulation data prove that the depletion effect promotes an accumulation of polymers in the center of real cavities or capsules. This phenomenon can be reduced by an increased

concentration, the higher chain stiffness, or by a weakly attractive surface.[21, 34] The quality of the solvent may also be important. The atomistic simulation of a single polyetyleneoxide (PEO) chain in a droplet revealed[4] that the PEO chain in acetonitrile settled in the interior of the droplet, in harmony with the above data. Conversely, in aqueous droplets, the PEO chain consistently resided near the droplet interior surface.

Chain contraction in bulk solution. Next, we examine an analogy between chains in a sphere and bulk solution near the overlap threshold. Earlier, a strong connection between these conditions of flexible self-avoiding polymers was pointed out.[17] A close packing of imaginary spheres in bulk solution in 3D space is reduced in 2D representation to the hexagonal stacking of spheres imitating the quasi-spherical confinement of a central chain (Figure 9). At $\varphi < \varphi^*$, the coils in bulk solution are more or less separated from each other. Still, the surrounding radially placed molecules may affect the conformation of the central molecule. At $\varphi \approx \varphi^*$, a similarity between polymers in a spherical confinement and bulk solution is quite conspicuous.

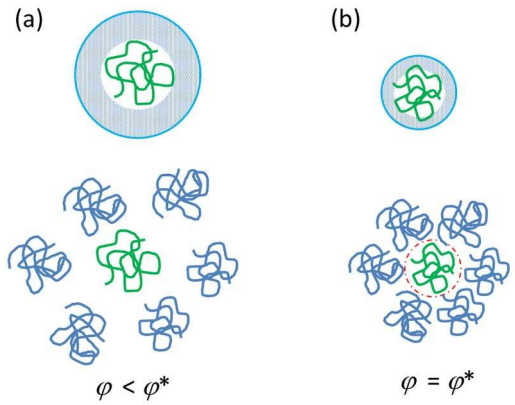

Figure 9. Schematic comparison of the space restraints on a polymer in a sphere and the central chain surrounded by hexagonally stacked chains slightly below φ^* (a), and at $\varphi \approx \varphi^*$ (b).

While the scaling description of polymer solution in bulk has gained wide acceptance, the issue of chain dimension at concentrations near the onset of the semidilute regime remains unsettled. The inspection of the numerous literature data prompts to an observation that the shrinking of chain size with increasing φ in bulk solution begins already below the threshold φ^*. The simulation reports[31-32, 35-36] suggest that this phenomenon is particularly noticeable in the unknotted and non-concatenated ring polymers of various chain lengths. Studies of polymer solutions under flow show that the chain shrinking below φ^* is additionally enhanced by the hydrodynamic interaction.[37-38] A reduction of R_g under φ^* can also be noticed in the results for single-chain nanoparticles in solution.[39] Besides, in measurements of the concentration dependence of fluorescence of polystyrene solutions, an unforeseen increase in fluorescence intensity in dilute solution was reported.[40] This observation was assigned to the weak interaction of polystyrene coils and their ensuing compaction at concentrations under φ^*.

We have chosen to contrast the data in Refs [31-32] about the shrinking of polymers in bulk solution with our data for the cavity-confined polymers. The bulk solution data for chains of various lengths[31-32] are precisely represented by the function $R_g/R_{g0} = (1+\alpha(\varphi/\varphi^*))^{\beta}$, where α and β are the parameters specific for the linear and ring polymers. The plots of $R_g(\varphi)$ in a bulk solution seen in Figures 4 and S2 confirm an excellent agreement between the two sets of data. These bulk solution data[31-32] show a small continuous decrease in the dilute regime that corroborates the existence of weak interaction at concentrations $\varphi < \varphi^*$. Due to this interaction, the radius of gyration of linear chains at overlap transition φ^* is reduced by 4% relative to R_{g0}, whereas in ring polymers this reduction amounts to 10% (Figures 4 and S2). Hence, the scaling theory assumption of the constant size $R_g = R_{g0}$ in the dilute regime should be considered as an approximation even in the case of bulk solutions.

The two examples of spherical constraints illustrated in Figure 9 differ primarily by the nature of the effective interaction energy. The strong hard-sphere repulsion between beads and the cavity surface gives rise to enormous free energy penalty F_{sph} forbidding coil penetration. This kind of strong interaction was originally predicted from the mean-field potential for two linear polymers in bulk solution[41] resulting in the effective penalty $F_{lin} \sim N^{1/5}kT$. In long polymers, the predicted penalty is so strong that coils should behave as practically impenetrable to each other. This estimation of the two-chain interaction was later corrected[42] by taking into account the monomer correlation. The analysis revealed[43] that the two-chain energy penalty F_{lin} is actually fairly weak, about 2 kT, allowing for an easy interpenetration of coils. A small, 4% impact of the neighboring stacked chains on the dimension of a central chain at $\varphi \approx \varphi^*$ in linear polymers in Figure 4 is consistent with the low value of the free energy F_{lin}.

On the other hand, the concentration shrinking $R_g(\varphi)$ in ring polymers is substantial, intermediate between those for the linear in bulk and confined polymers (Figure 4). This observation suggests that the interpenetration free-energy penalty F_{ring} should be larger than F_{lin} and lie somewhere between two extremities, $F_{lin} < F_{ring} << F_{sph}$. It is well known that the chain topology of ring polymers gives rise to their unique properties differing from the linear analogs. The ring polymers are subjected to topological constraints determined at the preparation stage due to concatenation and knotting.[44] In dilute solution two unlinked rings feel an entropic repulsion upon a close approach as the number of possible conformations is reduced due to non-concatenation.[44] Hence, on increasing concentration, the ring polymers tend to squeeze themselves instead of penetrating other chains. The entropic repulsion specific to ring polymers affects the free-energy penalty F_{ring} and can be determined from the effective interaction potential that in ring polymers possesses apart from the positive steric term (common with the linear

chains), also an extra topological term.[45] Since the latter term is also positive, this estimation confirms that the mutual interpenetration of ring polymers is more difficult than the linear ones.

The role of the topological interaction increases with concentration, and in the semidilute solution, the ring polymers assume a collapsed non-Gaussian conformation. As a result, the shrinking of the size of ring chains in bulk scales with the exponent x = -0.295 in the power law $R_g \sim \varphi^x$ (Figure 4), in deviation from x = -0.125 predicted by the scaling theory and validated in the linear polymers.[31,32] The slopes of the concentration shrinking of the ring polymers in a cavity and bulk solution in Figure 4 are comparable, and both are slightly smaller than the limit of x = -0.33 for the dense globule. The correspondence in the scaling exponent for chain shrinking is a compelling sign that the condensed conformations occurring in semidilute solutions of ring polymers in bulk and a cavity are comparable.

CONCLUSIONS

The single-chain simulations in the paper are concentrated on three issues: (a) the shrinking of polymer dimensions in a cavity, (b) the polymer depletion in a repulsive sphere, and (c) the similarity between chain squeezing in a cavity and that in bulk solution at the threshold φ^*. Firstly, the simulation data present evidence that the confinement of flexible linear and ring polymers into a sphere leads to a gradual crossover from a dilute to a semidilute regime. The chain size at the overlap concentration φ^* is by about 40 % contracted for both topologies as compared with that at infinite dilution. These observations are not consistent with the scaling theory predictions of the constant chain size R_{g0} in the dilute regime, and a discontinuous dilute-semidilute crossover.

Next, it was shown that the concentration-induced chain squeezing is amplified by the emergence of the depletion layer. A new formula is proposed to compute the thickness of the depletion layer δ in a cavity. In the dilute regime, a large part (up to two-thirds) of the total sphere volume is barely accessible to polymer segments. The depletion effect induces a substantial difference between the local polymer concentration far away from the cavity surface and the average concentration considered in the scaling theory.

Finally, we have contrasted the squeezing of a polymer in a sphere with a parallel situation of the quasi-spherical stacking of coils in bulk solution near the threshold φ^*. The recapitulated literature data provide evidence of weak interaction of polymers in the dilute regime neglected in the scaling theory. We have identified a systematic tendency of chain size reduction at threshold φ^* in bulk solution. The shrinking of coils in solution near φ^* is qualitatively like that observed in a cavity. The size contraction of about 10 % found in ring polymers in bulk is midway between those for the linear in bulk and 3D confined polymers. Different intensities of chain squeezing tendency in a sphere and bulk are linked to the free-energy penalty of penetration of surrounding barriers.

The above findings advance the present understanding of polymer solutions under 3D confinement and will find use in the interpretation of experiments with the hard- and soft-shell particles and cavities in nanoscience and biomedicine. A prominent example is an array of box-like cavities based on silicon wafers used in experiments to probe the organization of trapped polymers.[46]

ASSOCIATED CONTENT

Supporting Information

The supplementary graphs describe polymer squeezing and the depletion effect in a cavity (PDF).

AUTHOR INFORMATION

Corresponding author

Tomáš Bleha - Polymer Institute, Slovak Academy of Sciences, 84541 Bratislava, Slovakia orcid.org/0000-0003-3292-0189; Email: upoltble@savba.sk

Author

Peter Cifra - Polymer Institute, Slovak Academy of Sciences, 84541 Bratislava, Slovakia orcid.org/0000-0003-2075-4179; Email: cifra@savba.sk

Notes

The authors declare no competing financial interests.

ACKNOWLEDGMENT

This work was supported by the VEGA Grants 2/0102/20 and 2/0038/24. Furthermore, P.C. would like to acknowledge the contribution of COST Action CA17139.

REFERENCES

1. Bialas, F.; Reichinger, D.; Becker, C. F. W., Biomimetic and biopolymer-based enzyme encapsulation. *Enzyme Microb. Technol.* **2021,** *150*, 109864.

2. Kato, A.; Shindo, E.; Sakaue, T.; Tsuji, A.; Yoshikawa, K., Conformational Transition of Giant DNA in a Confined Space Surrounded by a Phospholipid Membrane. *Biophys. J.* **2009,** *97* (6), 1678-1686.

3. Rideau, E.; Dimova, R.; Schwille, P.; Wurm, F. R.; Landfester, K., Liposomes and polymersomes: a comparative review towards cell mimicking. *Chem. Soc. Rev.* **2018,** *47* (23), 8572-8610.

4. Oh, M. I.; Consta, S., Charging and Release Mechanisms of Flexible Macromolecules in Droplets. *J. Am. Soc. Mass Spectrom.* **2017,** *28* (11), 2262-2279.

5. Arsene, M.-L.; Răut, I.; Călin, M.; Jecu, M.-L.; Doni, M.; Gurban, A.-M., Versatility of Reverse Micelles: From Biomimetic Models to Nano (Bio)Sensor Design. *Processes* **2021,** *9* (2), 345.

6. Lee, N.-K.; Johner, A., Polymers grown in cavities: Vesicles and droplets. *J. Chem. Phys.* **2019,** *150* (16) 164905.

7. Shin, J.; Cherstvy, A. G.; Metzler, R., Polymer Looping Is Controlled by Macromolecular Crowding, Spatial Confinement, and Chain Stiffness. *ACS Macro Letters* **2015,** *4* (2), 202-206.

8. de Gennes, P.-G., *Scaling Concepts in Polymer Physics*. Cornell University ed.; Ithaka, NY: 1979.

9. Teraoka, I., *Polymer solutions: an introduction to physical properties*. J. Wiley ed.; New York: 2002.

10. Daoud, M.; De Gennes, P.-G., Statistics of macromolecular solutions trapped in small pores. *J. Phys. France* **1977,** *38*, 85-93.

11. Grosberg, A. Y.; Khokhlov, A. R., *Statistical Physics of Macromolecules*. American Institute of Physics ed.; New York, 1st edn. 1994.

12. Teraoka, I.; Wang, Y., Computer simulation studies on overlapping polymer chains confined in narrow channels. *Polymer* **2004,** *45*, 3835–3843.

13. Wang, Y., Confinement free energy and chain conformations of homopolymers confined between two repulsive walls. *J.Chem. Phys.* **2004,** *121* (8), 3898-3904.

14. Jorge, S.; Rey, A., Conformational properties of flexible polymer chains in highly confined environments. *J.Chem. Phys.* **1997,** *106* (13), 5720-5730.

15. Cifra, P., Channel confinement of flexible and semiflexible macromolecules. *J. Chem. Phys.* **2009,** *131*, 224903.

16. Cacciuto, A.; Luijten, E., Self-Avoiding Flexible Polymers under Spherical Confinement. *Nano Lett.* **2006,** *6* (5), 901-905.

17. Jun, S.; Arnold, A.; Ha, B.-Y., Confined Space and Effective Interactions of Multiple Self-Avoiding Chains. *Phys. Rev. Lett.* **2007,** *98* (12), 128303.

18. Cifra, P.; Bleha, T., Free Energy of Polymers Confined in Open and Closed Cavities. *Macromol. Theory Simul.* **2012,** *21*, 15-23.

19. Sakaue, T., Semiflexible Polymer Confined in Closed Spaces. *Macromolecules* **2007,** *40* (14), 5206-5211.

20. Cifra, P.; Bleha, T., Pressure of Linear and Ring Polymers Confined in a Cavity. *J. Phys. Chem. B* **2023,** *127* (20), 4646-4657.

21. Lekkerkerker, H. N. W.; Tunier, R., *Colloids and the Depletion Interaction*. Springer: 2011.

22. Sakaue, T.; Raphaël, E., Polymer Chains in Confined Spaces and Flow-Injection Problems:Some Remarks. *Macromolecules* **2006,** *39*, 2621-2628.

23. Bleha, T.; Cifra, P., Compression and Stretching of Single DNA Molecules under Channel Confinement. *J. Phys. Chem. B* **2020,** *124* (9), 1691-1702.

24. Cifra, P.; Bleha, T., Piston Compression of Semiflexible Ring Polymers in Channels. *Macromol. Theory Simul.* **2021,** *30* (5), 2100027.

25. Wang, Y.; Tree, D. R.; Dorfman, K. D., Simulation of DNA Extension in Nanochannels. *Macromolecules* **2011,** *44*, 6594–6604.

26. Jin, Z.; Zhao, S.; Wu, J., Entropic forces of single-chain confinement in spherical cavities. *Phys. Rev. E* **2010,** *82* (4), 041805.

27. Bleha, T.; Cifra, P., Energy/entropy partition of force at DNA stretching. *Biopolymers* **2022,** *113* (5), e23487.

28. Benková, Z.; Cifra, P., Simulation of Semiflexible Cyclic and Linear Chains Moderately and Strongly Confined in Nanochannels. *Macromolecules* **2012,** *45*, 2597−2608.

29. Jun, S.; Wright, A., Entropy as the driver of chromosome segregation. *Nature Reviews Microbiology* **2010,** *8* (8), 600-607.

30. Polson, J. M., Polymer translocation into and out of an ellipsoidal cavity. *J. Chem. Phys.* **2015,** *142* (17), 174903.

31. Reigh, S. Y.; Yoon, D. Y., Concentration Dependence of Ring Polymer Conformations from Monte Carlo Simulations. *ACS Macro Lett.* **2013,** *2* (4), 296-300.

32. Cai, X.; Liang, C.; Liu, H.; Zhang, G., Conformation and structure of ring polymers in semidilute solutions: A molecular dynamics simulation study. *Polymer* **2022,** *253*, 124953.

33. Fleer, G. J.; Skvortsov, A. M.; Tuinier, R., Mean-Field Equation for the Depletion Thickness. *Macromolecules* **2003,** *36* (20), 7857-7872.

34. Bleha, T.; Cifra, P., Depletion potential between two attractive plates mediated by polymers. *Polymer* **2005,** *46* (24), 10996-11002.

35. Lang, M.; Fischer, J.; Sommer, J. U., Effect of Topology on the Conformations of Ring Polymers. *Macromolecules* **2012,** *45* (18), 7642-7648.

36. Narros, A.; Likos, C. N.; Moreno, A. J.; Capone, B., Multi-blob coarse graining for ring polymer solutions. *Soft Matter* **2014,** *10* (48), 9601-9614.

37. Huang, C.-C.; Winkler, R. G.; Sutmann, G.; Gompper, G., Semidilute Polymer Solutions at Equilibrium and under Shear Flow. *Macromolecules* **2010,** *43* (23), 10107-10116.

38. Weiss, L. B.; Likos, C. N.; Nikoubashman, A., Spatial Demixing of Ring and Chain Polymers in Pressure-Driven Flow. *Macromolecules* **2019,** *52* (20), 7858-7869.

39. Moreno, A. J.; Lo Verso, F.; Arbe, A.; Pomposo, J. A.; Colmenero, J., Concentrated Solutions of Single-Chain Nanoparticles: A Simple Model for Intrinsically Disordered Proteins under Crowding Conditions. *J. Phys. Chem. Lett.* **2016,** *7* (5), 838-844.

40. Qin, L.; Li, L.; Sha, Y.; Wang, Z.; Zhou, D.; Chen, W.; Xue, G., Conformational Transitions of Polymer Chains in Solutions Characterized by Fluorescence Resonance Energy Transfer. *Polymers* **2018,** *10* (9), 1007.

41. Flory, P. J.; Krigbaum, W. R., Statistical Mechanics of Dilute Polymer Solutions. II. *J. Chem. Phys.* **1950,** *18* (8), 1086-1094.

42. Grosberg, A. Y.; Khalatur, P. G.; Khokhlov, A. R., Polymeric coils with excluded volume in dilute solution: The invalidity of the model of impenetrable spheres and the influence of excluded volume on the rates of diffusion-controlled intermacromolecular reactions. *Makromol. Chem., Rapid Commun.* **1982,** *3* (10), 709-713.

43. Louis, A. A.; Bolhuis, P. G.; Hansen, J. P.; Meijer, E. J., Can Polymer Coils Be Modeled as ``Soft Colloids"? *Phys. Rev. Lett.* **2000,** *85* (12), 2522-2525.

44. Sakaue, T., Topological free volume and quasi-glassy dynamics in the melt of ring polymers. *Soft Matter* **2018,** *14* (36), 7507-7515.

45. Chubak, I.; Likos, C. N.; Smrek, J., Topological and threading effects in polydisperse ring polymer solutions. *Mol. Phys.* **2021,** *119* (19-20), e1883140.

46. Capaldi, X.; Liu, Z.; Zhang, Y.; Zeng, L.; Reyes-Lamothe, R.; Reisner, W., Probing the organization and dynamics of two DNA chains trapped in a nanofluidic cavity. *Soft Matter* **2018,** *14* (42), 8455-8465.

Supporting Information: Continuous crossover from the dilute to semidilute concentration regime in spherically confined polymers

Peter Cifra and Tomáš Bleha[*]

Polymer Institute, Slovak Academy of Sciences, 84541 Bratislava, Slovakia

In this Supporting Information, we present a few of additional figures. The figures broaden the analysis and support the conclusions arrived at in the main text.

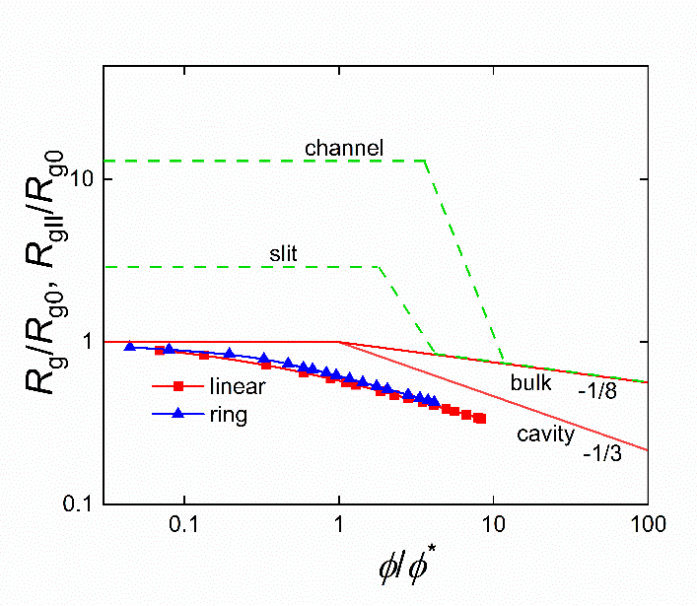

Figure S1. Logarithmic plot of the variation of the size of flexible polymers with concentration as predicted by the scaling theory for solution in bulk and in a cavity (characteristic slopes are indicated). The simulation data for linear polymers in a sphere (symbols) are also included. The related predictions of the longitudinal component of the radius of gyration R_{g0ll}/l for the slit and channel (dashed lines) are drawn schematically, not to the scale. Adapted from Ref.[1]

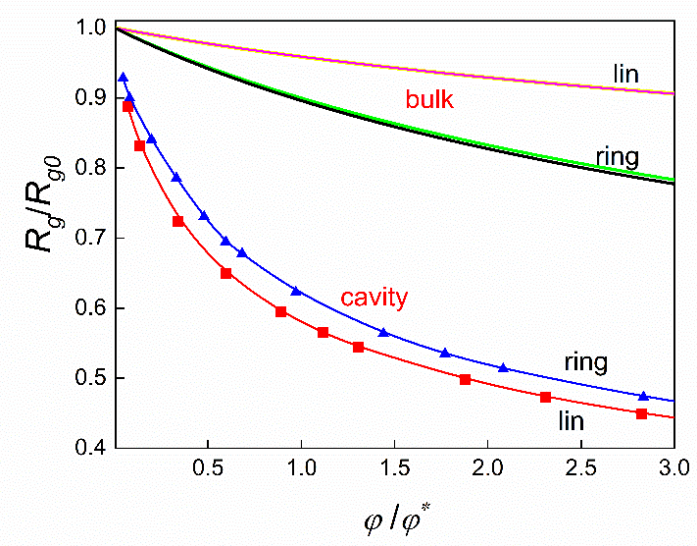

Figure S2. The linear representation of the dependence of the chain size on concentration from simulations of the linear (red squares) and ring (blue triangles) polymers in a sphere plotted using the reduced variables R_g/R_{g0} and φ/φ^*. In addition, the data from the related simulations of polymers in bulk solution[2-3] are included, represented by the function $R_g/R_{g0} = (1+\alpha(\varphi/\varphi^*))^x$, where $\alpha = 0.4$; $x = -0.125$ (yellow) and $\alpha = 0.43$; $x = -0.295$ (green) apply for linear and ring polymers, respectively in Ref.[2] and $\alpha = 0.38$; $x = -0.13$ (magenta) and $\alpha = 0.45$; $x = -0.295$ (black) in Ref.[3]

(a) (b)

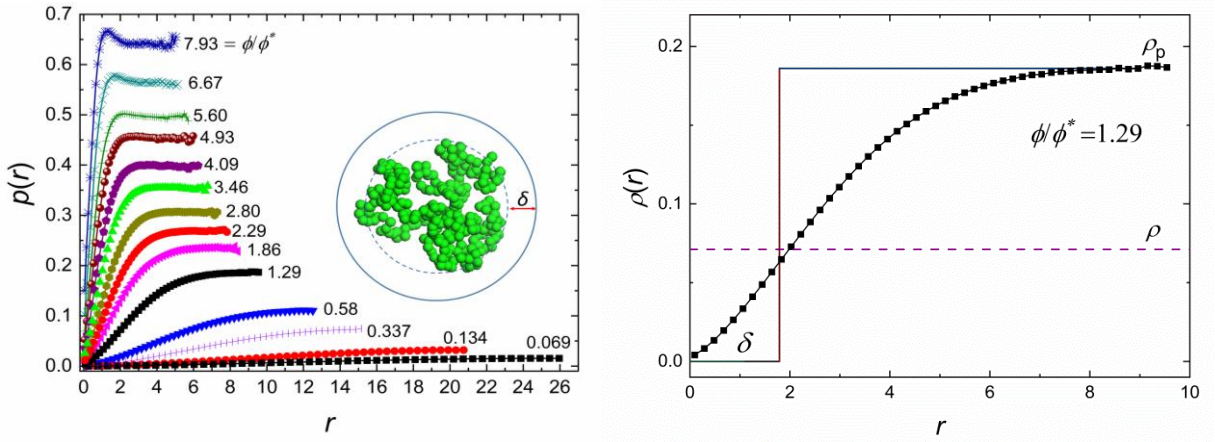

Figure S3. (a) The radial density profiles $\rho(r)$ of a flexible linear polymer in a cavity at the reduced concentrations φ/φ^* given in the legend based on the effective bond length $l = 0.71$ used in simulation. (b) A representation of the simulation profile for $\varphi/\varphi^* = 1.29$ (symbols) by the step function. The depletion length δ is computed from eq (1). The dashed line shows the average numerical density ρ.

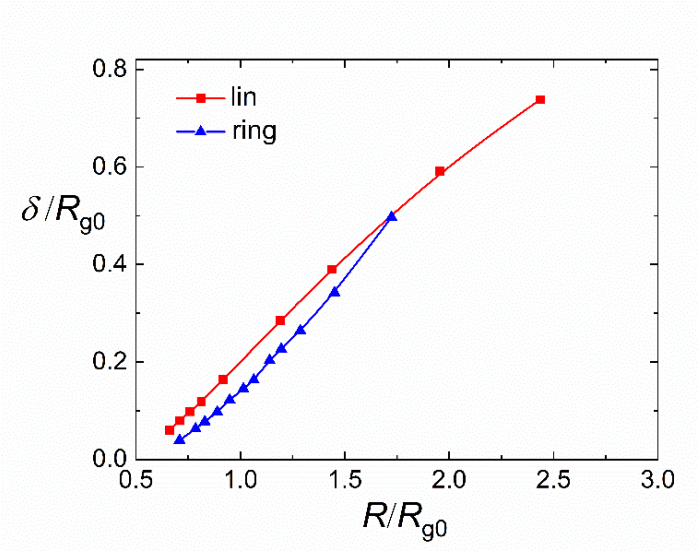

Figure S4. Dependence of the depletion thickness δ normalized by unconfined chain size R_{g0} as a function of the reduced radius of a sphere R.

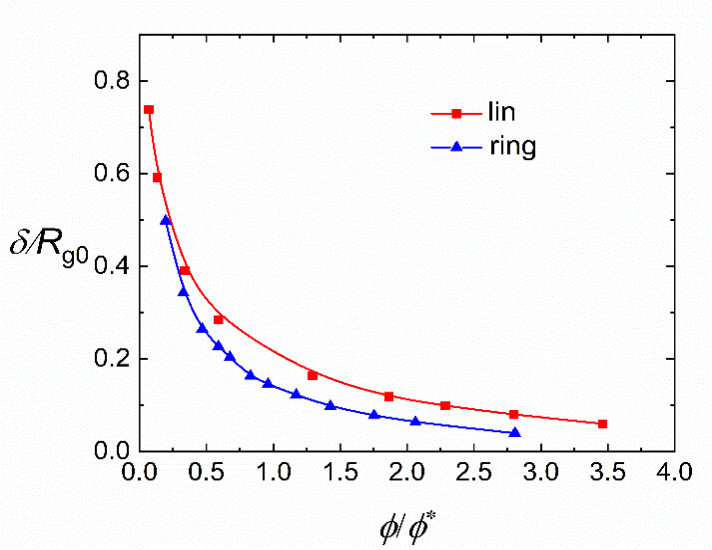

Figure S5. Dependence of the depletion thickness normalized by unconfined chain size R_{g0} as a function of the reduced concentration φ/φ^*.

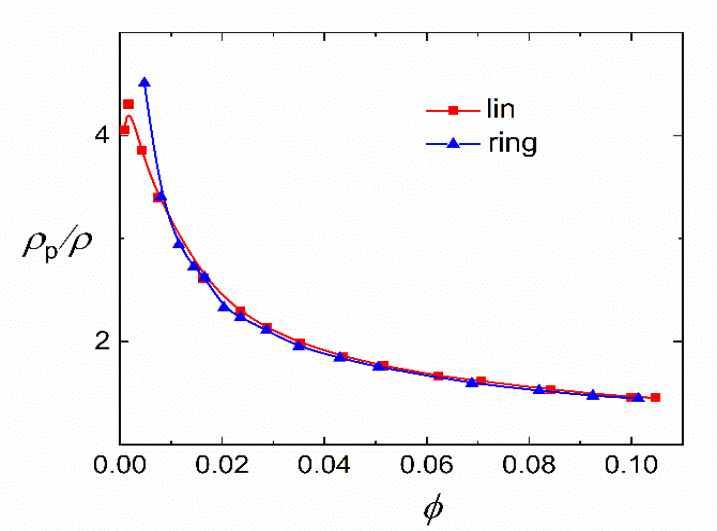

Figure S6. The plot of the ratio $\rho_p/\rho = \varphi_p/\varphi$ of the numerical or volume concentrations at the profile plateau to the respective average concentrations as a function of the concentration $\varphi = \rho v_1$ for linear and ring polymers inside a sphere.

References

1. Teraoka, I.; Wang, Y., Computer simulation studies on overlapping polymer chains confined in narrow channels. *Polymer* **2004,** *45*, 3835–3843.

2. Reigh, S. Y.; Yoon, D. Y., Concentration Dependence of Ring Polymer Conformations from Monte Carlo Simulations. *ACS Macro Lett.* **2013,** *2* (4), 296-300.

3. Cai, X.; Liang, C.; Liu, H.; Zhang, G., Conformation and structure of ring polymers in semidilute solutions: A molecular dynamics simulation study. *Polymer* **2022,** *253*, 124953.